Aging Effects on the Phase Composition and Chain Mobility of Isotactic Poly(propylene)

Cristian Hedesiu,* Dan E. Demco,* Ralf Kleppinger, Geert Vanden Poel, Klaas Remerie, Victor M. Litvinov, Bernhard Blümich, Rieky Steenbakkers

Changes in phase composition and chain mobility in injection-molded isotactic poly(propylene), crystallized from the melt with slow cooling rate and subsequently quenched, associated with aging at temperature well above T_g for 150 and 1 000 h, are studied using time-domain ^{1}H solid-state NMR and XRD. All sample exhibit physical aging when exposed to elevated temperatures, and the physical aging kinetics was observed to depend on the morphology of the homopolymer iPP and aging temperatures. The significant increase in the tensile modulus in time was observed for injection-molded iPP. The observed property changes induced by aging are attributed to microstructural changes within the semi-rigid and amorphous fractions.

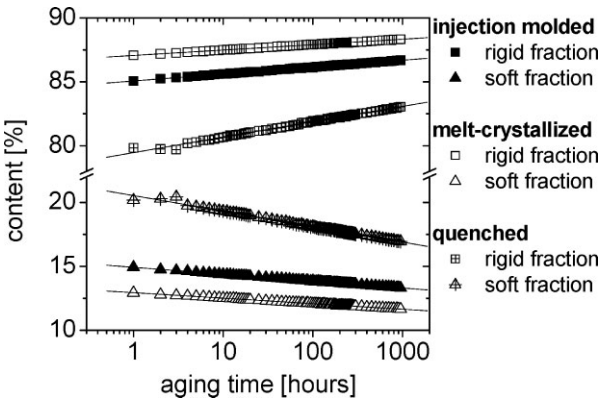

Introduction

Physical aging of semi-crystalline polymers, which has been studied extensively in the past from many aspects, refers to the evolution toward an equilibrium state and the associated changes in the morphological organization and physical properties at temperatures between the glass transition temperature and melting temperature.[1–7] The physical aging at different temperatures and different times involves the densification of the amorphous fraction (reduction in free volume),[8] constraints in the chain mobility,[9] lamellar perfection or densification, lamellar thickening, crystallization of constrained polymer chains forming small crystals or fringed micelles, and partial melting-recrystallization. The exact origin of the changes in isotactic poly(propylene) (iPP) samples (and in other semi-crystalline polymers) with aging time and aging temperature is still in dispute.[1–9] One reason for the dispute lies in the limitations of different techniques used to probe the structure of these materials.

DSC rarely provides values for crystallinity that are similar to those from other techniques.[10,11] Wide-angle X-ray diffraction (WAXD) requires an estimation of the amorphous halo and the lattice imperfection factor[12] and small-angle X-ray diffraction (SAXS) is largely model dependent.[13] It should be noted that the problem with SAXS analyses are enhanced in the case of iPP, due to the cross-hatched lamellar morphology.[14]

One important feature for aging behavior that is generally agreed upon by researchers is whether the

C. Hedesiu, K. Remerie, R. Steenbakkers
SABIC Europe BV, P.O. Box 319 6160 AH, Geleen, The Netherlands
E-mail: cristian.hedesiu@SABIC-europe.com
D. E. Demco
DWI an der RWTH Aachen e.V. and Institute of Technical and Macromolecular Chemistry at RWTH Aachen,
Pauwelsstr. 8, D-52056 Aachen, Germany
E-mail: demco@mc.rwth-aachen.de
R. Kleppinger, G. V. Poel, V. M. Litvinov
DSM Research, P.O. Box 18, 6160 MD Geleen, The Netherlands
B. Blümich
Institut für Technische und Makromolekulare Chemie, Rheinisch-Westfälische Technische Hochschule, Worringer Weg 1, D-52056 Aachen, Germany

DOI: 10.1002/mame.200800140

annealing temperatures are above or below the crystalline dielectric α_c relaxation. The crystalline α_c relaxation is associated with the rotational/translational motion traveling along the crystal stem that can grow from the soft fraction in a crystal thickening process.[15–18] In ref.[18] it was shown that, for iPP, the polymer chains perform helical jumps about the helix axis in the crystalline domains at temperature above 360 K. The most probable mechanism for an increase in crystallinity due to aging is secondary crystallization, in which new lamellae are inserted between those formed during the primary crystallization. This mechanism occurs since the regions remaining amorphous still have the potential to partially crystallize. The newly-formed lamellae are constrained by those formed during primary crystallization. They are thicker because they are formed at higher temperatures. Because an additional driving force is needed, the newly-formed lamellae at lower temperature, upon further non-isothermal cooling, are thinner. They may thicken if a low temperature active process is plausible. It is not only a matter of aging temperature – with respect to the glass transition temperatures of the crystalline and amorphous phases – for the new formed lamella, but the aging also depends on the initial iPP morphology.

The first aim of this paper is to study in detail the effects of aging temperature and aging time on the phase composition, crystallinity, melting and crystallization temperatures, chain mobility and mechanical properties of injection-molded, slowly crystallized from a static melt, and quenched homopolymeric iPP by ^{1}H low-field solid-state NMR, DSC and X-ray methods. The second goal of this paper is to show that the ^{1}H low-field solid-state NMR relaxometry is capable of detecting small changes in the phase composition and chain mobility due to aging at different times and different temperatures. Moreover, a correlation between the changes in the NMR and DSC parameters caused by aging and mechanical data is presented and discussed.

Experimental Section

Sample and Heat Treatments

Sabic Europe grade name homopolymeric iPP was used in all investigations. The isotacticity was measured to be 98.5% by liquid state ^{13}C NMR. The stereochemical defects (atactic fraction) were approximately 1%. The additive package was calcium stearate and irganox. The material was characterized by a melt flow index of 10 g $\times$ (10 min)$^{-1}$. The first sample was injected-molded iPP using an Engel 45A machine. The melt temperature was set to 235 °C, the holding pressure to 40 MPa, the holding time to 20 s, the cooling time to 20 s and the overall cycle time to 49.5 s. The second sample was slowly crystallized from a static melt as follows: the injection-molded plates were melted at 230 °C for 30 min in an oven under nitrogen flow, in order to avoid the oxidation of the samples, and finally crystallized at a cooling rate of about 5 °C $\cdot$ min^{-1}. The third sample was quenched from the melt. The sample was brought to 250 °C, kept for 30 min at that temperature and then quenched from the melt at −195 °C between two metal plates.

Aging study was made at 28 °C for all the homopolymeric iPP samples. Moreover, the samples were further annealed in the NMR probe, for times between 10 min and 1 000 h after preparation. For the aging study in the temperature range from 70–130 °C, the melt-crystallized iPP samples were annealed in the NMR probe for times ranging from 10 min to 150 h. All NMR measurements were repeated with an interval of 1 h, keeping the samples in the NMR probe.

X-Ray Diffraction

WAXD experiments of starting and annealed samples were performed with a modified Kratky setup attached to a conventional, sealed X-ray tube (40 kV and 50 mA), which provided line-focused Ni-filtered Cu K_α radiation (0.154 nm). The scattering signal was recorded with an MBraun 50M position-sensitive detector. The calibration was performed as described in ref.[19]

DSC

DSC measurements were performed to investigate the influence of time/temperature treatment on the crystallization and melting behavior of homopolymeric PP samples. The applied temperature profiles are described below. All samples were kept for 15 min at 250 °C, then cooled at 10 °C $\cdot$ min^{-1} to 25 °C, held for 1 min at 25 °C and then heated at 10 °C $\cdot$ min^{-1} to 28, 70 and 130 °C, and kept for 10, 60, 120, 480 and 1 440 min at these programmed temperatures. This pre-treatment can be compared with the thermal treatment used to measure the PP samples by ^{1}H solid-state NMR. After this isothermal treatment, the samples were cooled at 10 °C $\cdot$ min^{-1} to 0 °C, held for 5 min to equilibrate before heating at 10 °C $\cdot$ min^{-1} to 200 °C (1st heating curve), kept for 5 min at this temperature and cooled at 10 °C $\cdot$ min^{-1} to 0 °C (cooling curve), held for 5 min to equilibrate before heating at 10 °C $\cdot$ min^{-1} to 200 °C (2nd heating curve). The so-called 1st heating curve provides information concerning the thermal treatment (a certain time at a certain temperature), whereas both the cooling curve and the 2nd heating curve are being used to verify whether or not the thermal treatment has influenced the

Macromol. Mater. Eng. 2008, 293, 847–857

Macromolecular Journals
DOI: 10.1002/mame.200800140

thermal response of the material, that is, has caused molecular and/or morphological changes.

Mechanical Measurements

Impact Testing Method

A single-point Izod test was used to measures the impact resistance of the investigated material. Izod impact strength is defined as the strength at which the specimen breaks when hit with a pointed hammer having a set kinetic energy. The specimen is notched to prevent its deformation upon impact. The tests were performed with a Zwick Type 5110 testing machine according to ASTM D256 on $65 \times 12.7 \times 3.2$ mm^3 specimens and with the striking speed of the hammer being 3.5 m $\cdot$ s^{-1}. The given value of the impact strength is an average of five tests. The impact strength a_{iN}, expressed in kJ $\cdot$ m^{-2} was calculated from the following equation:

$$a_{iN} = \frac{E_c}{h \cdot b_E} \times 10^3 \quad (1)$$

where E_c is the corrected energy (J) absorbed by breaking the specimen, h is the thickness of the specimen (mm) and b_N is the width at the notch (mm).

Two hammers were used, having kinetic energies of 2.75 and 5.5. If, after carrying out the test with the lighter hammer, the specimen did not fully break, the specimen was discarded without recording the impact strength and the heavier hammer was used instead.

Flexural Testing Method

The principle of this test is to bend or flex the specimen in the middle at a constant bending rate until the specimen fractures or until the deformation reaches some predetermined value. During the test, the force applied to the specimen is measured. The flexural modulus was computed and used as an indication of the material's stiffness when flexed.

The tests were carried out with a Zwick tensile machine according to ASTM D790. The dimensions of the specimen were $65 \times 12 \times 3.2$ mm^3. The values of flexural modulus are an average values of five tests.

Tensile Testing Method

Dog-bone shaped tensile bars with a length of 70 mm, thickness of 4 mm and gauge dimensions of 20 mm length were cut from iPP plates. The samples were uniaxially stretched using a Zwick Z050 tensile machine according to ISO 37-II to investigate the tensile behavior of the specimens and for determining the tensile strength and tensile modulus. The tests were performed at 25 °C with a deformation rate of 50 mm $\cdot$ min^{-1}.

NMR Measurements

Transverse magnetization relaxation (T_2 relaxation) experiments were used to study the changes in the phase composition and chain mobility in homopolymer iPP samples upon aging at different times and different temperatures. The experiments were performed at low magnetic field strength using a Bruker Minispec MQ20 spectrometer operating at a proton resonance frequency of 19.6 MHz. The data were collected for static samples at temperatures between 28 and 130 °C. The measurements, as a function of increasing aging temperature, were performed from 10 min after thermal stabilization time at each temperature. The duration of a 90° pulse was 2.7–2.8 μs, the dead time was 7 μs, and the dwell time was 0.5 μs. A BVT-3000 temperature controller was used for temperature regulation with temperature stability better than 1 °C. In order to measure the decay of the ^{1}H transverse magnetization (T_2 decay), the free induction decay (FID) was recorded each hour after a 90°-pulse excitation (SPE – single pulse excitation), that is, 90°_x – dead time – acquisition of the amplitude $A(t)$ of the transverse magnetization as a function of time t.

At 28 °C, the FID of homopolymer iPP samples was fitted with a linear combination of an Abragam and a Gaussian function:

$$A(t) = A(0)^{\text{rigid}} \exp\left[-\left(\frac{t}{T_2^{\text{rigid}}}\right)^2\right] \cdot \left[\frac{\sin(at)}{at}\right] + A(0)^{\text{soft}} \exp\left[-\left(\frac{t}{T_2^{\text{soft}}}\right)^2\right] \quad (2)$$

At higher temperatures, from 70 to 130 °C, the FID of homopolymer iPP samples was fitted with a linear combination of Abragam, Gaussian, and an exponential function:

$$A(t) = A(0)^{\text{rigid}} \exp\left[-\left(\frac{t}{T_2^{\text{rigid}}}\right)^2\right] \cdot \left[\frac{\sin(at)}{at}\right] + A(0)^{\text{semi-rigid}} \exp\left[-\left(\frac{t}{T_2^{\text{semi-rigid}}}\right)^2\right] + A(0)^{\text{soft}} \exp\left[-\left(\frac{t}{T_2^{\text{soft}}}\right)\right] \quad (3)$$

The parameter a is related to the second and fourth van Vleck moments. The transverse relaxation times (T_2), which are characteristic of different slopes in the magnetization decay curve, are related to the mobility of each fraction. The relative fractions of the relaxation components, $\{A(0)^k/[A(0)^{\text{rigid}} + A(0)^{\text{semi-rigid}} + A(0)^{\text{soft}}]\} \times 100\%$, represent the relative amounts of hydrogen atoms (mass

fractions) of iPP phases/fractions with different molecular mobility. Repeated experiments for the same sample indicated that the relative error of the extracted relaxation parameters was about 1%.

Results

Mechanical Results

To determine the influence of aging on the mechanical properties of homopolymer iPP, the effect of aging on the flexural modulus, impact strength, and shrinkage were investigated. Figure 1 shows the results of flexural modulus (parallel and perpendicular) plotted against the aging time. The iPP samples were aged at 28 °C. The modulus increases with aging time. Compared to the value reached after 1 h, the modulus has increased by approximately 13.5% after 200 h.

The decrease in impact strength in both directions (parallel and perpendicular), measured at 23 °C with aging time can be observed in Figure 2. Free shrinkage experiments were performed to investigate the changes of the organization of the amorphous phase depending on the aging time. Figure 3 shows the change of the degree of shrinkage in time. In general, the shrinkage behavior is non-linear and increases with increasing aging time.

X-Ray Results

The polymer chains, adopting a 3_1 helical conformation when crystallized from the melt, can attain various spatial arrangements that give rise to monoclinic α-, trigonal β- or orthorhombic γ-forms. The appearance of the different crystalline forms depends to a large extend on the chain microstructure,[20,21] processing conditions[22,23] and presence of specific nucleating agents.[24,25] However, under

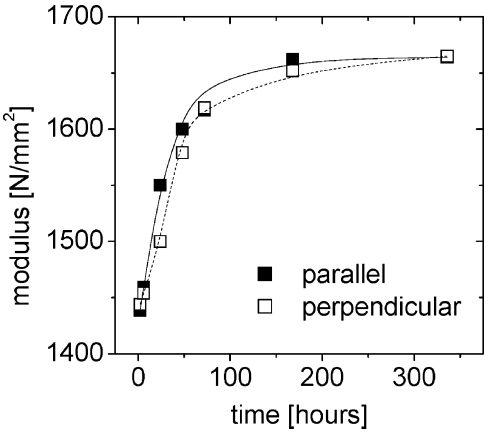

Figure 1. Flexural modulus as a function of aging time at 23 °C for injection-molded iPP samples.

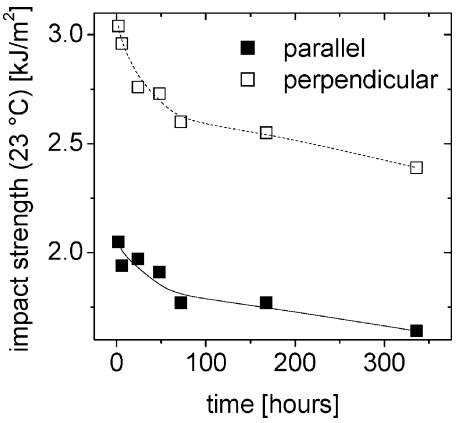

Figure 2. Izod impact strength in parallel and perpendicular directions at 23 °C as a function of aging time for injection-molded iPP samples.

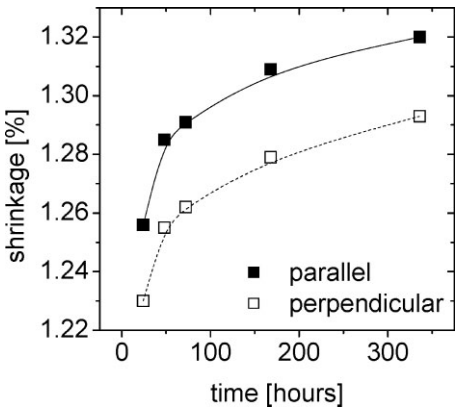

Figure 3. Relative shrinkage in parallel and perpendicular direction versus aging time for injection-molded iPP samples.

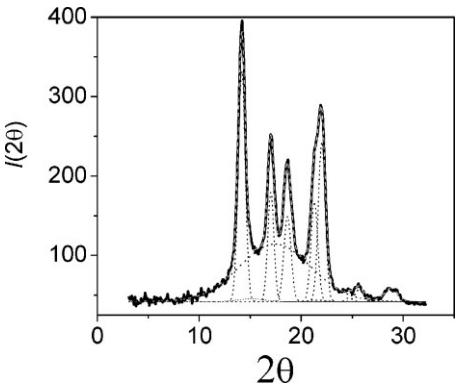

Figure 4. Deconvolution of 1-dimensional X-ray patterns for crystalline and amorphous phases of iPP crystallized from the melt with a low cooling rate.

Macromol. Mater. Eng. **2008**, *293*, 847–857

Macromolecular Journals
DOI: 10.1002/mame.200800140

conditions as usually applied during industrial processing the α-form is always predominant. WAXD studies directly reflect the molecular arrangement and possible changes induced in the crystalline phase due to different thermal history. From the position of the diffraction peaks in the X-ray pattern displayed in Figure 4, it is apparent that samples, obtained by applying moderate cooling rates in the absence of shear and nucleating agents, crystallize into the crystalline α-form with unit cell parameters of $a = 6.65$ Å, $b = 20.96$ Å, $c = 6.5$ Å, and $\beta = 99.8^{\circ}$. Samples rapidly quenched from the melt, on the other hand, reveal only two broad maxima due to short-range ordering perpendicular to the helical segments (Figure 5). This mesomorphic structure reveals a degree of ordering intermediate between the amorphous and crystalline phase, as already indicated by Natta and Corradini.[26] In general, the diffraction signal recorded from iPP subjected to different thermal history represents a superposition of contributions arising from amorphous, crystalline and mesomorphic phases. In order to separate these contributions, peak parameters extracted from Figure 4 and 5 were used as start parameters during subsequent fitting of the data sets. To demonstrate the changes in the arrangement of PP helices caused by thermal treatment, a quenched sample was successively annealed at increasing temperatures. The WAXD results displayed in Figure 6a reveal a gradual increase in the amount of the α-crystalline material with increasing annealing temperature, a finding that is reflected by the relative fractions of the different phases that are extracted from the XRD pattern (cf. Figure 6b). Within the time scale of our experiments the most pronounced changes appear to take place at temperatures above 70 °C. At this temperature, the amount of the mesomorphic phase in the material gradually decreases whereas the content of α-crystalline material is increasing, suggesting that the order among the helical segments tends to increase. Note, however, that a continuous decrease in the amount of amorphous phase from 70%

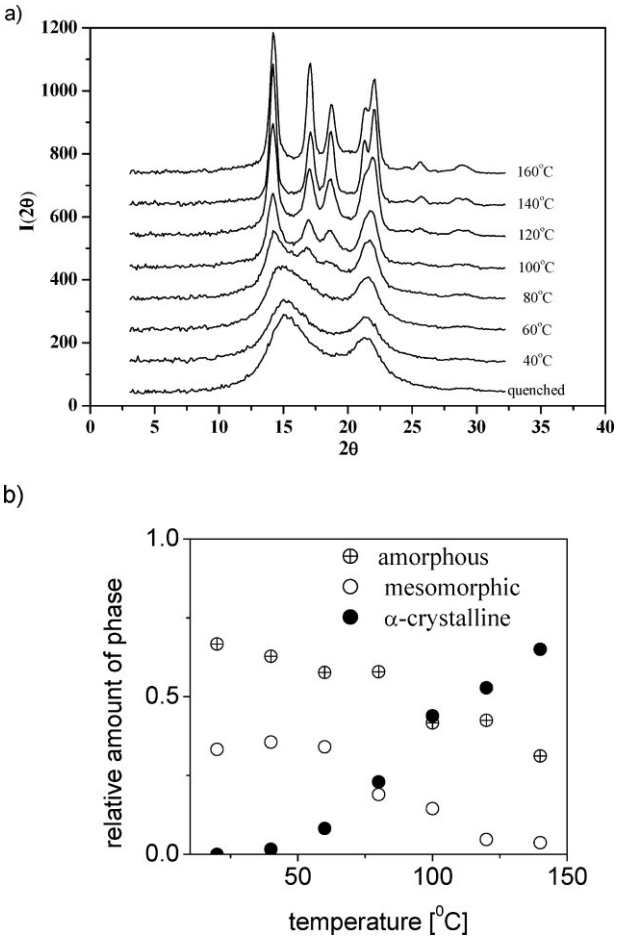

Figure 6. a) 1-dimensional X-ray pattern of quenched iPP samples recorded at different temperatures. b) The amount of crystalline, mesomorphic and amorphous phases of quenched iPP measured at different temperatures.

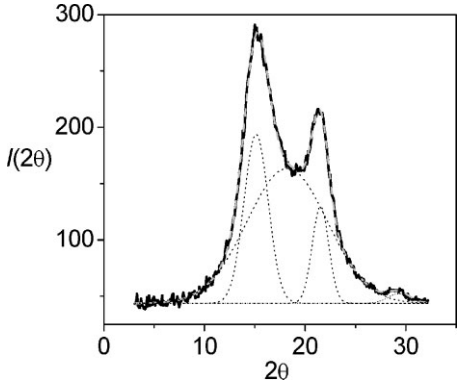

Figure 5. Deconvolution of 1-dimensional X-ray pattern of quenched iPP samples.

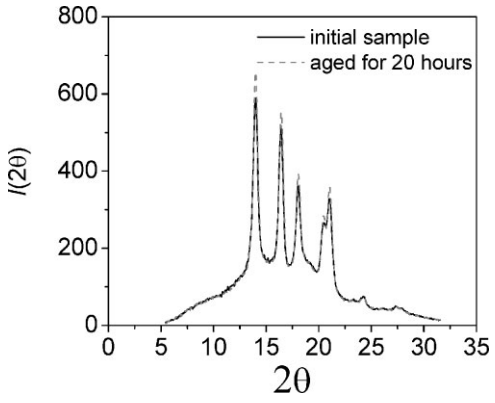

Figure 7. X-ray patterns of initial (10 min) and aged iPP samples.

down to 40% is observed within the entire temperature range.

Figure 7 shows the X-ray patterns of crystallized-from-the-melt iPP samples aged for 10 min and 20 h. Comparing the diffraction patterns of the samples aged for 10 min and 20 h, no significant differences were observed as a function of time in the lattice parameters. The D-spacing values are almost constant for the observed crystallographic planes, which indicate no changes in the crystal packing. The significant changes of the mechanical properties during aging cannot be attributed to the changes in the crystallinity, in agreement with the invariance of X-ray patterns at different aging times.

DSC Results

Isothermal Measurements

In the isothermal measurements, no crystallization phenomena could be detected. Although crystallization is present, the DSC does not record a heat signal during the isothermal treatment. The crystallization is so slow that it cannot be seen due to the noise of the baseline.

Dynamic Measurements

An offset and melting temperature, T_m^{1st}, can be calculated by the 1st heating curve. All results are presented in Table 1. In order to compare the thermally-annealed samples with non-treated iPP, offset and apparent offset temperatures were used, based on a previous article.[19] The crystallization temperature, T_c, the enthalpy of crystallization, ΔH_c and the melting temperature, T_m^{2nd}, (2nd heating curve), are also presented in Table 1. The enthalpy of the cooling curve was used to verify the reproducibility of the enthalpy of all samples. Table 1 shows that, by calculating the mean crystallization temperature, $T_{c,\ average} = 121.0 \pm 0.3\ ^\circ C$, the mean crystallization enthalpy, $\Delta H_{c,\ average} = 98 \pm 1\ J \cdot g^{-1}$ and the mean $T_m^{2nd} = 164.0 \pm 0.6\ ^\circ C$, one may conclude that the thermal treatment does not change the thermal response of the material after erasing the thermal history. The thermal treatment is a reversible process, which means that no structural changes took place within the homopolymeric iPP sample.

For the samples kept at 28 and 70 °C, it is very difficult to determine the T_{offset} due to the small specific heat capacity, C_p, step and the baseline curvature. Aging of the samples

Table 1. Changes in offset temperature, T_{offset}, crystallization temperature, T_c, the enthalpy of crystallization, ΔH_c, and melting temperature, T_m, of homopolymeric iPP samples as a function of aging time and aging temperature. Observations were made based on dynamic measurements for samples kept at 110–130 °C.

Time	Temp	T_{offset}	T_m^{1st}	T_c	ΔH_c	T_m^{2nd}
min	°C	°C	°C	°C	$J \cdot g^{-1}$	°C
5	0	–	162.9	121.2	100	163.3
10	130	132	164.1	120.9	98	164.2
60		133.4	164.9	121.3	97	164.7
120		133.7	164.8	121.1	97	164
480		134.2	164	120.5	98	163.2
1 440		134.9	164.8	120.6	98	163.7
10		74.4	164.2	120.9	98	164.4
60		75.7	163.8	121.4	98	164.4
120	70	78.3	163	120.7	99	164.2
480		77.1	162.9	120.7	99	163.2
1 440		80.5	164.2	120.8	97	164.3
10	28	31.4	163.9	121.1	98	164.2
60		34	164.7	121.1	97	165
120		35.8	164.2	121.1	98	164.5
480		36.9	163.3	121.4	98	163.8
1 440		40.2	162.8	121.5	98	164
Mean			163.9	121	98	164.0
Stand. dev.			0.7	0.3	1	0.5

Macromol. Mater. Eng. **2008**, *293*, 847–857

Macromolecular Journals
DOI: 10.1002/mame.200800140

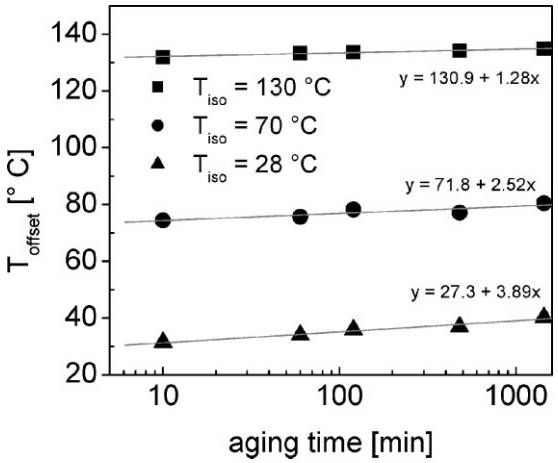

Figure 8. Offset temperature values as a function of log(aging time) for iPP samples annealed at different temperatures.

causes a shift of the melting temperature towards higher temperatures. That defines the offset temperature. The offset temperature of the transition related to the thermal treatment seems to shift to higher temperatures when longer isothermal annealing is applied at this isothermal temperature (Table 1). The offset temperature values are plotted as a function of the log(aging time) and the data are linearly fitted (Figure 8). The slope of these lines present the variation of the offset temperature with time, which is the largest for the sample kept isothermal at the lowest temperature (28 °C). The offset temperature differences between 1 440 and 10 minutes at a well-defined temperature (130, 70 and 28 °C) are presented in Table 2. The lower the applied isothermal temperature, the larger the difference is of the offset temperature (slope in Figure 8). These results clearly indicate long-term changes when keeping homopolymeric PP samples for long time at a constant temperature. The changes are recorded as an increase of the C_p, which may indicate that the amorphous phase is changing, rather than the crystalline phase. Most likely, the amorphous and rigid-amorphous phases are seriously influenced by annealing time and temperature effects.

Table 2. Offset temperature difference between 1 440 and 10 min for annealing of PP samples at 28, 70, and 130 °C.

Temperature	$\Delta[T_{1\,440} - T_{10}]$
°C	°C
130	2.9
70	6.1
28	8.8

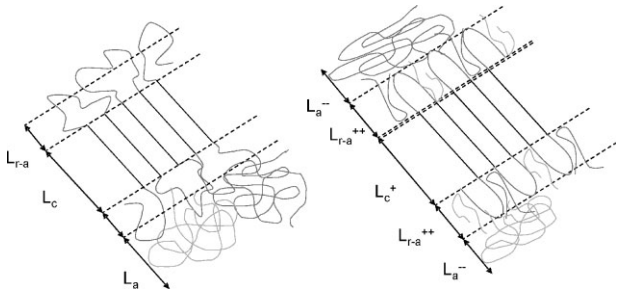

Figure 9. Simplified schematic representation of the changes in the morphology of homopolymeric iPP due to aging/annealing. The morphology before and after aging is shown on the left- and right-hand sides, respectively.

Figure 9 presents a hypothetical picture showing how annealing influences the amorphous (L_a), rigid-amorphous ($L_{r\text{-}a}$) and crystalline phases (L_c). After annealing, the amount of rigid-amorphous phase increases, L_{r-a}^{++}, amorphous phase decreases, L_a^{--}, and the crystalline phase increases slightly, L_c^{+} (3% crystallinity increase), with time/temperature changes. These results are in line with the observed NMR results (*vide infra*).

NMR Results

Changes in the Phase Composition and Chain Mobility upon Aging at 28 °C

Analyses of FID of injection-molded, crystallized-from-the-melt, and quenched iPP samples in terms of rigid and soft fractions were performed at a temperature of 28 °C, not far above the T_g of the amorphous phase (0 °C). At this temperature, we are claiming that the contrast in chain mobility of the rigid and soft fractions of iPP is enhanced, and the aging process at this temperature can be followed over time with high sensitivity. The high amount of the rigid fraction detected by NMR at 28 °C is due to the contribution of the immobilized soft fraction to the amount of the crystalline phase. Aging at 28 °C for 1 000 h causes an approximately 1–2 wt.-% increase in the amount of the rigid fraction at the expense of the soft fraction (Figure 10a). For all iPP samples, the measured amounts of the rigid phase increases linearly with increasing logarithm of aging time (Figure 10a). The gradual changes in the phase composition show that the aging at 28 °C persists for long times.

The chain mobility of the rigid fractions (T_2^{rigid}) of iPP is hardly affected by aging at 28 °C for 1 000 h, whereas the chain mobility in the soft fraction (T_2^{soft}) decreases over time (Figure 10b). A decrease in the chain mobility in the soft fraction due to the aging was also observed by Agarwal et al.[27] and VanderHart et al.[28]

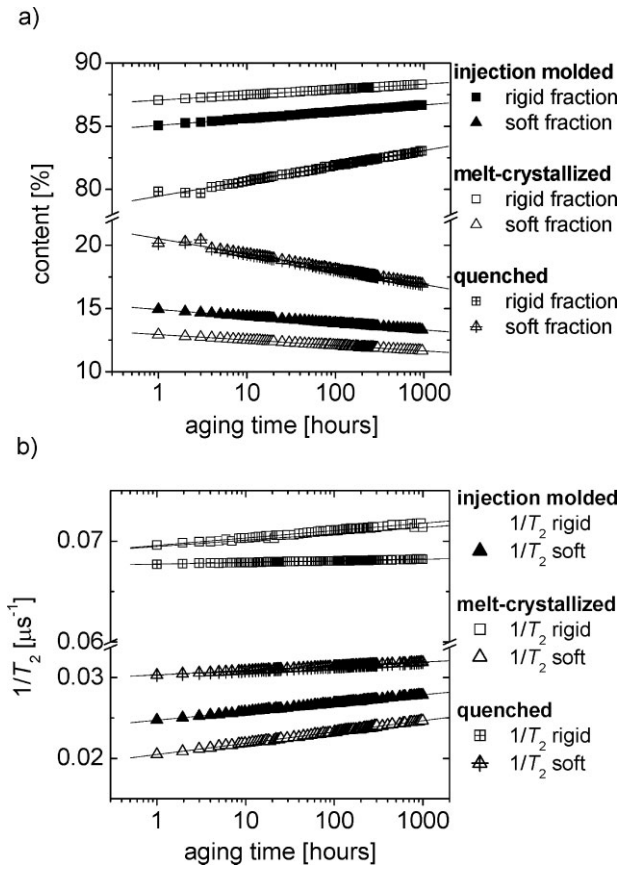

Figure 10. a) The amounts of rigid (% T_2^{rigid}) and soft (% T_2^{soft}) fractions of both injection-molded and crystallized-from-the-melt homopolymer iPP samples as a function of the annealing time at 28 °C. b) The effect of the annealing at 28 °C on chain mobility, as determined by the T_2 relaxation time for the different fractions of both injection-molded and melt-crystallized iPP. Larger amplitude and/or frequency of molecular motions lead to longer T_2 values.

To calculate a relative rate of aging, the amounts and chain mobility ($1/T_2^{rigid}$, $1/T_2^{soft}$) were plotted against aging time on a logarithmic scale, and a linear fit was made to the data. The changes in the phase content and chain mobility due to the aging at 28 °C are approximately linear in logarithmic scale over aging time during the 1 000 h of our observation. The overall slopes observed in Figure 10a are not much different for both injection-molded (slope = 0.53 μs^{-1}), melt-crystallized (slope = 0.42 μs^{-1}) and quenched (slope = 1.2 μs^{-1}) iPP samples. In the case of chain mobility in soft fractions, the difference in the slopes are larger (Figure 10b).

Changes in the Phase Composition and Chain Mobility upon Aging at 70–130 °C

At temperatures between 70 and 130 °C, the proton NMR free induction decay (FID) for iPP samples crystallized from the melt can be decomposed into three components. They are assigned to three fractions with different chain mobilities, manifested in the transverse magnetization times: the rigid (T_2^{rigid}), semi-rigid ($T_2^{semi-rigid}$), and soft (T_2^{soft}) fractions. At elevated temperatures, the contrast in the chain mobility between the rigid, semi-rigid and soft fractions of all iPP samples is enhanced and a quantitative analysis can be performed suggesting the three-phase

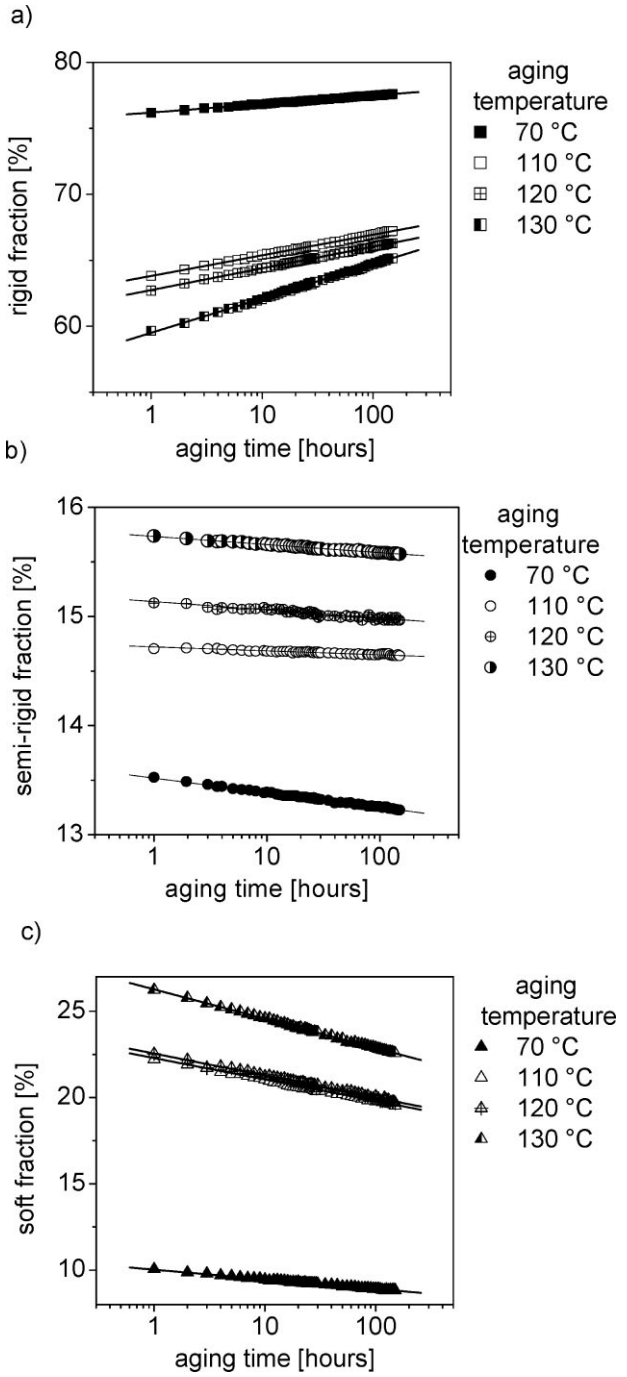

Figure 11. The amount of a) rigid (% T_2^{rigid}), b), semi-rigid (% $T_2^{semi-rigid}$), and c) soft fractions (% T_2^{soft}) of iPP crystallized from the melt as a function of the aging times and aging temperatures.

Macromol. Mater. Eng. **2008**, *293*, 847–857

Macromolecular Journals
DOI: 10.1002/mame.200800140

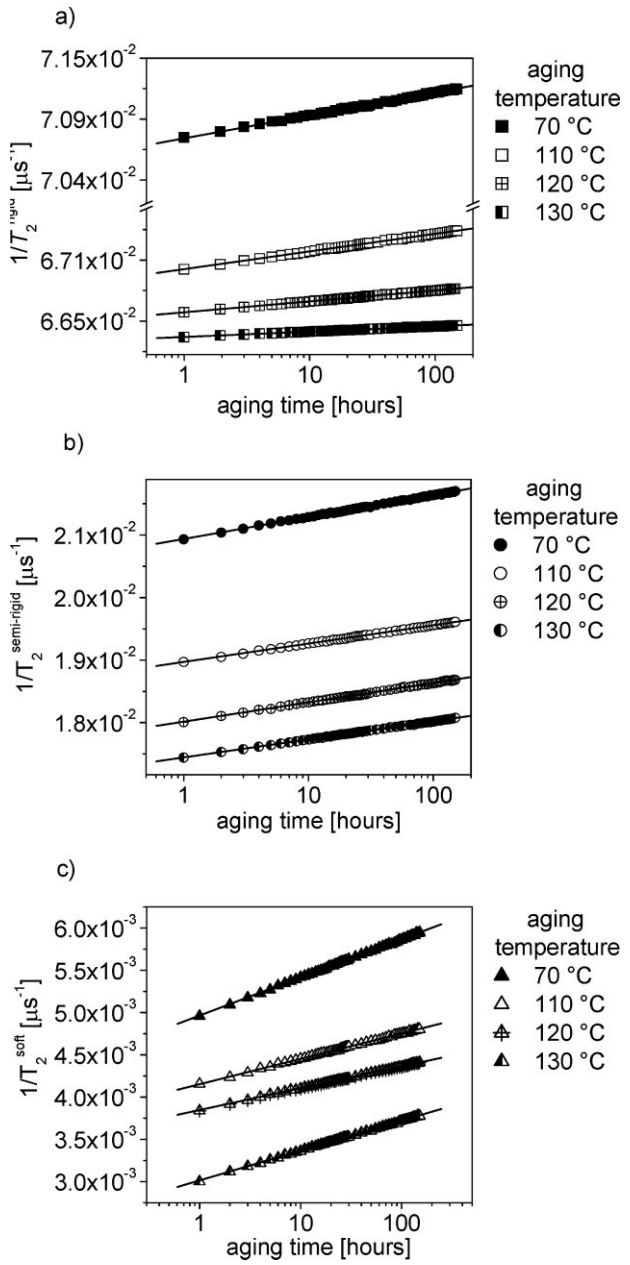

Figure 12. The effect of aging time and aging temperatures on chain mobility in a) rigid (T_2^{rigid}), b) semi-rigid ($T_2^{semi-rigid}$), and c) soft (T_2^{soft}) fractions of melt-crystallized iPP.

model. Aging in the temperature range from 70 to 130 °C for 150 h causes an approximately 1–2 wt.-% increase in the amount of the rigid fraction at the expense of the soft fraction (Figure 11) of the samples. The amount of the semi-rigid fraction remains almost constant in all the cases (Figure 11b). For all aging temperatures a decrease in the chain mobility of semi-rigid and soft fractions is observed (Figure 12). The chain mobility in the rigid fraction is much less influenced by aging time, particularly at high aging temperatures (Figure 12a).

Table 3. Slopes of the dependences at different aging temperatures of the rigid, semi-rigid, and soft fractions on log(aging time) (cf. Figure 11).

Aging Temp.	Slope		
°C	Rigid	Semi-rigid	Soft
70	0.28	−0.05	−0.32
110	0.68	−0.02	−0.63
120	0.71	−0.03	−0.64
130	1.13	−0.03	−0.88

Using the same approach as for samples aged at 28 °C, it is possible to calculate a relative rate of aging, at different aging temperatures, in terms of the slopes of the amounts graphs of the rigid and soft fractions versus log(aging time) (Figure 11), and the plots of T_2^{rigid}, $T_2^{semi-rigid}$, and T_2^{soft} versus log(aging time) (Figure 12). All the plots yield a nearly linear relationship at a function of log(aging time). The results obtained from those plots are summarized in Table 3 and 4.

Discussion

Physical Aging in Homopolymer iPP Samples

Our previous paper[19] reported that the morphology of iPP at temperature well above glass transition can be described using a three-phase (fractions) model, consisting of rigid, semi-rigid and soft phases. At temperatures close to 25 °C, the morphology of iPP can be described using a two-fraction model, rigid and soft amorphous fractions. The amount and chain mobility in each fraction are important parameters related to physical and mechanical properties of iPP sample. Those quantities typically change when the sample is exposed to temperatures well above

Table 4. Slopes of the dependences at different aging temperatures of the chain mobility ($1/T_2$) in the rigid, semi-rigid, and soft fractions on log(aging time) (cf. Figure 12).

Aging Temp.	Slope		
	Rigid	Semi-rigid	Soft
°C	10^{-5}	10^{-4}	10^{-4}
70	0.93	1.2	1.8
110	0.73	1.02	1.21
120	0.45	1.08	1.05
130	0.30	1	1.4

the glass transition due to physical aging.[29–37] It is known that the aging of iPP samples after fabrication causes changes in the structure and properties of the materials. The observed changes in the mechanical properties (Figure 1–3) with aging time indicate that micro-structural reorganization takes place within the material. An increase in flexural modulus has been observed (Figure 1), while impact strength decreases (Figure 2) with increasing aging time. The decrease in the impact strength could be associated with increasing of the amount of the rigid fraction during aging. Property changes occurring on aging are generally attributed to the relaxation process in the amorphous phase, leading to a reduction in free volume as determined by shrinkage (Figure 3). The mechanical data imply that the aging is restricting the motion of the polymer chains, and a good way of probing such changes is to study isothermally the changes in the ^{1}H NMR signal for a long period of time.

As shown above (Figure 10), when the sample after preparation is exposed to a temperature of 28 °C for 1 000 h the amount of the rigid fraction gradually increases over time, at the expense of the soft fraction. In contrast to the characteristic values describing the mechanical behavior, the increase in the amount of the rigid fraction is not very pronounced and is not sufficient to attribute the significant enhancement of mechanical properties during aging just to the secondary crystallization. The chain mobility of the rigid fraction remains almost constant and the chain mobility of the soft fraction decreases in time.

Based on information from Figure 10b, it is plausible to conclude that the aging at 28 °C influences mainly the soft fraction of all iPP samples prepared by different procedures, and the soft fraction is becoming more restricted probably due to molecular ordering. Our observations are in line with Struik's model.[38] The information provided by Figure 10 indicates that the aging rate is higher in the case of melt-crystallized homopolymer iPP, compared to injection-molded and quenched iPP samples. From these results, we can conclude that the important factors determining aging are the morphology of the sample, and a relationship between the physical aging kinetics and the relative amounts of the soft fraction existing in homopolymer iPP samples. We note that, at a temperature of 28 °C, we cannot make conclusions about the changes in the semi-rigid fraction due to aging, because at this temperature the NMR signal can be decomposed into only two components.

In order to study the changes in the semi-rigid fraction due to aging, an aging and NMR experiment was conducted in the temperature range 70–130 °C. Upon increasing the aging temperature from 28 to 70–130 °C, the frequency of molecular motions increases, which might lead to faster structural rearrangements. According to the results shown in Figure 12, it seems plausible to conclude that, in crystallized-from-the-melt iPP samples, the physical aging influences both the semi-rigid and soft fractions. These changes could be due to the formation of small crystals – secondary crystallization – as detected by WAXD. These crystals impose additional constraints on the mobility of the soft fraction. Based on chain mobility considerations, the formation of new crystals, due to secondary crystallization, takes place mainly in the semi-rigid and soft fractions, where the chain mobility decreases with increasing the aging time. Based on the results from Table 4, the aging rate increases with increasing aging temperature.

The results from the NMR, DSC and X-ray studies and mechanical properties point out that the structural changes are associated with two different phenomena: a molecular rearrangement, generally similar to secondary crystallization, accompanied by a decrease in segmental chain mobility of the amorphous chains involved in the diffusion process, and relaxation of a residual stress resulting from non uniform plastic flow occurring during injection-molding and quenching. A decrease in the segmental chain mobility, by increasing the structural packing density in the amorphous or intercrystalline regions due to the aging, results in an increase of the flexural modulus (cf. Figure 1.). As it was discussed in ref.[39] for PP and other semi-crystalline polymers, the crystalline regions act in part like cross-links, thereby tending to increase the modulus by increasing the resistance to deformation of the amorphous or semi-rigid regions. The effect of the formations of small crystals due to the secondary crystallization and immobilization of the amorphous phase is to cause the modulus to increase.

Conclusion

In this work, we have investigated the influence of morphology, aging time, and aging temperature on the physical aging behavior of iPP samples. We characterized the morphology in terms of the two- and three-phase model, comprising rigid and soft phases, and rigid, semi-rigid and soft phases, respectively. Injection-molded, crystallized-from-the-melt, and quenched iPP samples provided us with specimens of widely differing morphologies. Crystallization from the melt resulted in a relatively low amount of the soft fraction. This is consistent with a lower degree of constraint imposed by the crystallites on the mobility of the non-crystalline chain segments when crystallization occurs under conditions of high segmental mobility.

The extent and kinetics of physical aging in these samples were characterized by following the changes in the phase content and chain mobility with time. These changes in the amounts of the rigid, semi-rigid, and soft

Macromol. Mater. Eng. 2008, 293, 847–857

Macromolecular Journals
DOI: 10.1002/mame.200800140

fractions, and chain mobility in each fraction ($1/T_2^{rigid}$, $1/T_2^{semi-rigid}$ and $1/T_2^{soft}$) reveal a linear dependence on log(aging time). The changes in the phase content and chain mobility with time indicated that the extent of physical aging in semi-crystalline iPP is significant and easily quantifiable.

We have observed that the chain relaxation rate in semi-crystalline homopolymeric iPP is sensitive to the relative amounts of the semi-rigid and soft factions. Specifically, for a given aging history, the chain relaxation rate was observed to increase in the samples with a more stable morphology. This observation raises the possibility that the aging takes place primarily in regions of highest mobility that are more distant from the fold surface of the primary crystallites. The observations reported here also suggest that the conformational entropic state of the semi-rigid and soft fractions is relevant to physical aging in semi-crystalline polymers, as well as the proximity of the aging temperature to their glass transition temperatures.

Physical aging must be considered as an important factor when semi-crystalline iPP samples are designed for use in applications that involve prolonged exposure to above-ambient temperatures.

Received: May 9, 2008; Revised: July 23, 2008; Accepted: July 23, 2008; DOI: 10.1002/mame.200800140

Keywords: aging; isotactic poly(propylene) (PP); proton NMR transverse relaxation; SAXS

[1] N. G. McCrum, *Polymer* **1984**, *25*, 299.
[2] C. K. Chai, N. G. McCrum, *Polymer* **1980**, *21*, 706.
[3] P. E. Tomlins, *Polymer* **1996**, *37*, 3907.
[4] P. E. Tomlins, B. E. Read, *Polymer* **1998**, *39*, 355.
[5] T. C. Uzomah, S. C. O. Ugbolue, *J. Appl. Polym. Sci.* **1997**, *65*, 625.
[6] A. O. Ibhadon, *J. Appl. Polym. Sci.* **1996**, *62*, 1843.
[7] S. Hellinck, *Colloid Polym. Sci.* **1997**, *275*, 116.
[8] H.-H. Song, R.-J. Roe, *Macromolecules* **1987**, *20*, 2723.
[9] M. Agarwal, J. M. Schultz, *J. Polym. Eng. Sci.* **1981**, *21*, 776.
[10] J. R. Isasi, L. Mandelkern, M. J. Galante, R. G. J. Alamo, *Polym. Sci. Polym. Phys. Ed.* **1999**, *37*, 323.
[11] H. Zhou, G. L. Wilkes, *Polymer* **1997**, *38*, 5735.
[12] W. Ruland, *Acta Crystallogr.* **1961**, *14*, 1180.
[13] F. J. Balta-Calleja, C. G. Vonk, "*X-ray Scattering of Synthetic Polymers*", Elsevier, New York 1989.
[14] R. H. Olley, D. C. Bassett, *Polymer* **1989**, *30*, 399.
[15] R. H. Boyd, *Polymer* **1985**, *26*, 323.
[16] R. H. Boyd, *Polymer* **1985**, *26*, 1123.
[17] K. Schmidt-Rohr, H. W. Spiess, *Macromolecules* **1991**, *24*, 5288.
[18] D. Schaefer, H. W. Spiess, U. W. Suter, W. W. Fleming, *Macromolecules* **1990**, *23*, 3431.
[19] C. Hedesiu, D. E. Demco, R. Kleppinger, G. Vanden Poel, W. Gijsbers, B. Blümich, K. Remerie, V. M. Litvinov, *Macromolecules* **2007**, *40*, 3977.
[20] C. De Rosa, F. Auriemma, C. Spera, G. Talarico, O. Tarallo, *Macromolecules* **2004**, *37*, 1441.
[21] C. De Rosa, F. Auriemma, M. Paolillo, L. Resconi, I. Camurati, *Macromolecules* **2005**, *38*, 9143.
[22] R. Somani, B. S. Hsiao, A. Nogales, H. Fruitwala, S. Srinivas, A. H. Tsou, *Macromolecules* **2001**, *34*, 5902.
[23] K. Cho, D. N. Saheb, J. Choi, H. Yang, *Polymer* **2002**, *43*, 1407.
[24] J. Ščudla, M. Raab, K. J. Eichhorn, A. Strachota, *Polymer* **2003**, *44*, 4655.
[25] M. Blomenhofer, S. Ganzleben, D. Hanft, H. W. Schmidt, M. Kristiansen, P. Smith, K. Stoll, D. Mäder, K. Hoffmann, *Macromolecules* **2005**, *38*, 3688.
[26] G. Natta, P. Corradini, *Nuovo Cimento Suppl.* **1960**, *15*, 40.
[27] M. K. Agarwal, K. E. Helf, *Kolloid Z.* **1962**, *180*, 114.
[28] D. L. VanderHart, C. R. Snyder, *Macromolecules* **2003**, *36*, 4813.
[29] M. Hikosaka, K. Amano, S. Rastogi, A. Keller, *Macromolecules* **1997**, *30*, 2067.
[30] R. G. Alamo, G. M. Brown, L. Mandelkern, A. Lehtinen, R. Paukkerri, *Polymer* **1999**, *40*, 3933.
[31] A. Akizadeh, L. Richardson, J. Xu, S. McCartney, H. Marand, Y. W. Cheung, S. Chum, *Macromolecules* **1999**, *32*, 6221.
[32] H. Marand, A. Alizadeh, R. Farmer, R. Desai, V. Velikov, *Macromolecules* **2000**, *33*, 3392.
[33] M. Iijima, G. Strobl, G. *Macromolecules* **2000**, *33*, 5204.
[34] P. Maiti, M. Hikosaka, K. Yamada, K. A. Toda, F. Gu, *Macromolecules* **2000**, *33*, 9069.
[35] W. P. Weglarz, H. Peemoeller, A. Rudin, *J. Polym. Sci., Part B: Polym. Phys.* **2000**, *38*, 2487.
[36] A. Alizahedh, S. Sohn, J. Quinn, H. Marand, L. C. Shank, H. D. Iler, *Macromolecules* **2001**, *34*, 4066.
[37] T. Labor, C. Gauthier, R. Seguela, G. Vigier, Y. Bomal, G. Orange, *Polymer* **2001**, *42*, 7127.
[38] L. C. E. Struik, *Polymer* **1987**, *28*, 1521.
[39] A. V. Tobolsky, "*Structure and Properties of Polymers*", Interscience, New York 1965.